Studies of cracking behavior in melt-processed YBCO bulk superconductors

2006 J. Phys.: Conf. Ser. 43 429

(http://iopscience.iop.org/1742-6596/43/1/107)

Institute of Physics Publishing Journal of Physics: Conference Series **43** (2006) 429–433
doi:10.1088/1742-6596/43/1/107 7th European Conference on Applied Superconductivity

Studies of cracking behavior in melt-processed YBCO bulk superconductors

S. Haindl[1], H. W. Weber[1], M. Sefciková[2], K. Zmorayová[2], P. Diko[2], N. Hari Babu[3], D. A. Cardwell[3], L. Shlyk[4], G. Krabbes[4]

[1] Atomic Institute of the Austrian Universities, Stadionallee 2, 1020 Vienna, Austria
[2] Institute of Experimental Physics, Slovak Academy of Sciences, Watsonova 47, 04353 Košice, Slovak Republic
[3] IRC in Superconductivity, University of Cambridge, Cambridge, Madingley Road, Cambridge, CB3 0HE, UK
[4] Institute of Solid State and Materials Research Dresden, IFW Dresden, PO Box 270116, 01171 Dresden, Germany

E-mail: shaindl@ati.ac.at

Abstract. An important phenomenon in bulk superconductors fabricated by top-seeded-melt growth (TSMG) is the formation of cracks due to the inherent brittleness of the $YBa_2Cu_3O_{7-\delta}$ (Y-123) phase matrix. These form during the fabrication of the superconducting monolith and play an important role in the limitation of current flow. However, cracks may also form during cooling cycles of the sample to liquid nitrogen temperatures. In this investigation, macrocracks along the *c*-direction, in particular were analyzed microscopically before and after cooling. In addition we attempt to resolve the *c*-axis macrocrack formation pattern using the magnetoscan technique.

1. Introduction

In continuation of efforts [1,2] to clarify the cracking behavior of melt processed bulk superconductors, a combined experimental investigation has been made using optical microscopy and the magnetoscan technique. We concentrate on the *c*-axis macrocrack network, which represents a mesoscopic defect in bulk superconductors fabricated by the top seeded melt growth (TSMG) and limits the local supercurrent density in the sample. The formation of a dense network of *c*-axis macrocracks after oxygenation at around 400 °C supports the release of residual stresses and, therefore, prevents the bulk from fatal crack formation [1-2]. Additional cracks are formed by cooling the sample to 77 K and/or by the Lorentz forces present during magnetization and Hall probe mapping of the flux density distribution, employed commonly for sample characterization. Only the influence of the former on the generation of microcracks was investigated in the present study.

The magnetoscan technique [3] avoids the problem of cracking during magnetization, since the sample is characterized via the supercurrents that are induced locally by a small permanent magnet of comparatively low induction. It has been demonstrated in earlier work [4-8] that the magnetoscan technique can be used to identify growth sectors (GS) and growth sector boundaries (GSBs), corresponding to growth-induced inhomogeneities, the localization of small defects, such as cracks and grain boundaries, and partially oxygenated regions in the surface of superconducting monoliths. In

addition, magnetoscans show locally varying low signal patterns, which are distributed uniformly across the whole surface of the bulk, and which therefore require improved resolution for detailed investigation. Furthermore, the original magnetoscan system does not generate completely satisfactory results near the edges of a sample and is, therefore, less useful for characterizing small samples. Finally, the *c*-axis macrocracks have a typical spacing of ~ 35 μm, which is far beyond the resolution of the original magnetoscan system. Initial results on an improved magnetoscan design [9] are addressed in Section 2.

2. Experimental Details

Two bulk samples of YBCO fabricated by TSMG were investigated in this study. It was important to ensure that the samples had not been cooled previously to liquid nitrogen temperatures, in order to establish the influence of cooling cycle on the *c*-axis crack formation. Optical microscopy was performed on the as-processed, oxygenated samples, therefore, both before and after several cooling cycles.

2.1. Sample Preparation

Sample *C1* was fabricated at the IRC in Cambridge from a starting powder of Y-123 + 30 mol.% Y_2O_3 + 2.5 mol.% $Y_2Ba_4CuNbO_y$ + 0.1 wt.% Pt. A small Nd-Ba-Cu-O melt textured grain was used to seed the melt growth process. The pressed pellet was heated to 1045 °C, held there for 1 hour, cooled rapidly to 1005°C, cooled to 975°C at a rate of 0.5°C/h and, finally furnace cooled to room temperature. The sample was annealed under flowing oxygen at a temperature of 450°C for 100 hours. The fully processed sample had a diameter of 13.2 mm and a thickness of 5.9 mm. Sample *C2* was fabricated at IFW Dresden using a modified melt-crystallization process [10]. Commercial powders of Y-123, Y_2O_3, CeO_2 and ZnO, each of at least 99.99% purity, were used as precursors. The powders were mixed from a starting composition Y-123 + 0.3 Y_2O_3 + x (Zn concentration), where x = 0.5 at.%; [the at.% concentration is related to the formula $YBa_2(Cu_{100-x}Zn_x)_3O_7$]. Up to 1 wt.% Ce was added to refine the secondary Y-211 phase. The powders were ball milled and pressed into pelltes of diameter 30 mm after grinding. A $SmBa_2Cu_3O_{7-\delta}$ seed crystal was mounted on the top surface of the pellet with its *a/b* plane parallel to the sample surface. After the melt processing the sample was annealed in flowing oxygen at 380°C for 300 hours. The fully processed sample had a diameter of 26 mm and a thickness of 10.8 mm.

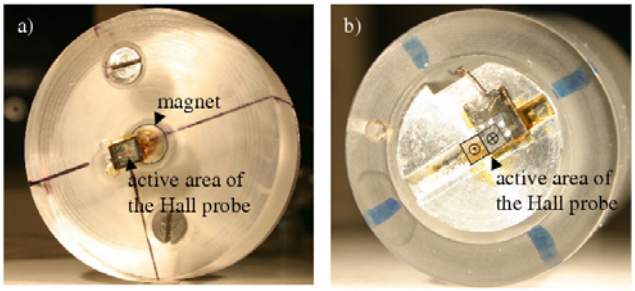

Fig. 1: a) Original magnetoscan arrangement. b) New magnetoscan design using two permanent magnets.

2.2. Magnetoscan: Original and modified design

In the original magnetoscan design, a HHP-VU Hall probe (AREPOC) was used to scan the sample surface immediately behind a permanent magnet of diameter of 6 mm (Fig. 1a). In the new design a HHP-VC Hall probe (AREPOC) is mounted at the edge between two small magnets (each 2 × 2 × 1 mm^3) with opposing directions of magnetization. The scans were performed in liquid nitrogen with a

distance of 0.2 mm between the sample surface and the Hall probe using scan grids of 0.25 × 0.25 mm² and of 0.20 × 0.20 mm². The Hall voltage was measured by a Keithley DMM with, a Hall probe current of 10 mA, supplied by a Lake Shore constant current source.

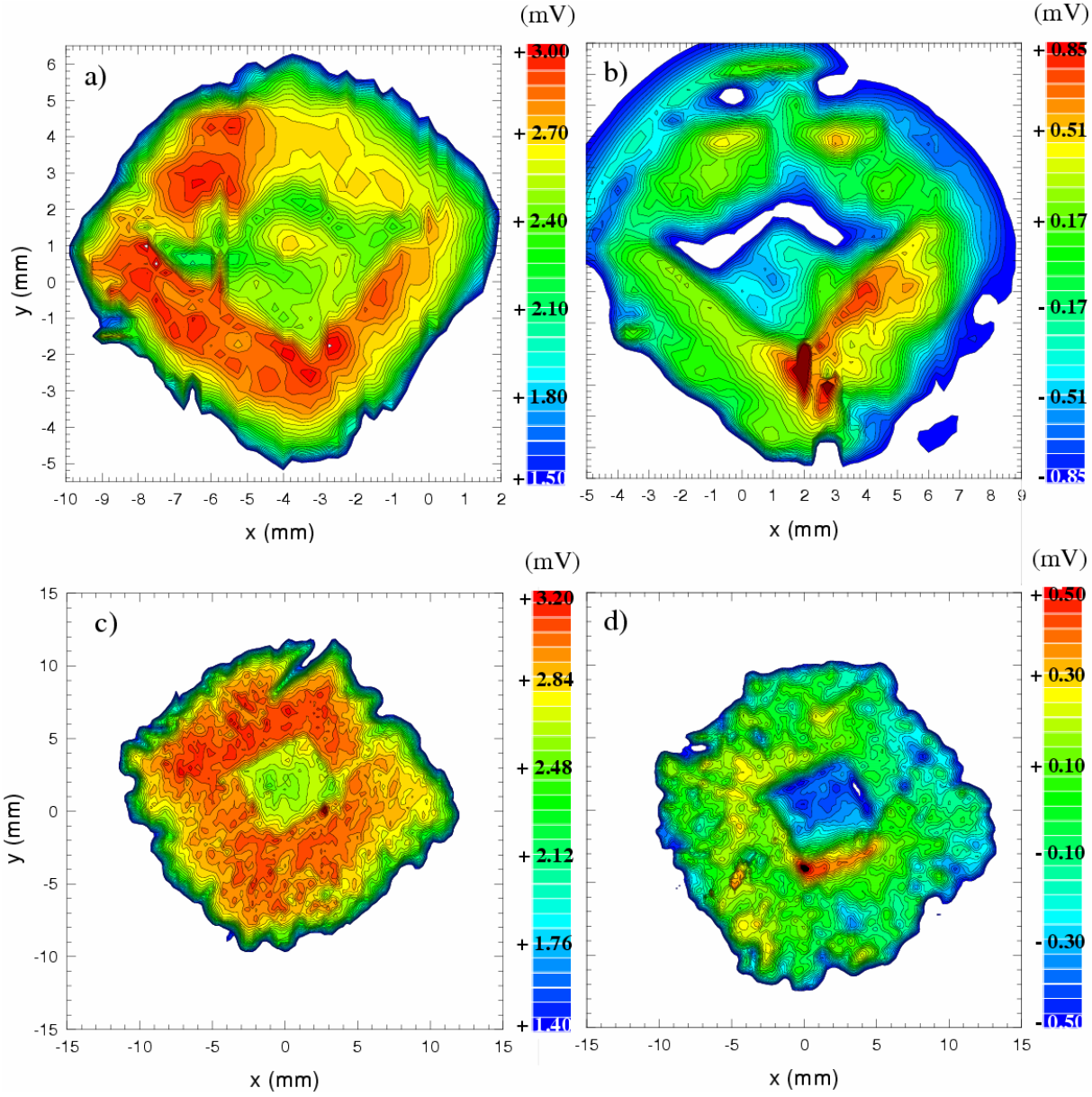

Fig. 2: a) Magnetoscan (original design, absolute scale) of sample *C1*. b) Magnetoscan (new design, relative scale) of sample *C1*. c) Magnetoscan (original design, absolute scale) of sample *C2*. d) Magnetoscan (new design, relative scale) of sample *C2*.

2.3. Optical Microscopy

The top surfaces of the TSMG bulks were carefully grinded on a set of SiC grinding papers and then polished. The *c*-axis cracks became visible after etching in a solution of 0.5 wt.% HCl in ethylalcohole. The spacing and length of the *c*-axis cracks were measured from micrographs taken using an optical microscope and an image processing software.

3. Results and Discussion

Magnetoscan results of samples *C1* and *C2* are presented in Fig. 2. Using the modified magnetoscan design a dipole-like behavior (i.e. a pattern of consecutive maxima/minima) of the signal is observed at a defect site (i.e. where the local density of *c*-axis cracks is higher). The corresponding signal from the original system, however, displays the magnetic induction generated by locally circulating supercurrents, which are reduced or even impeded by defects and weak links [11].

The *c*-axis crack structure was observed to be unchanged, when the optical micrographs of the virgin samples were compared with those taken after cooling during the magnetoscan. As a result, it can be concluded that a temperature cycle to 77 K does not introduce additional *c*-axis cracks into the sample microstructure.

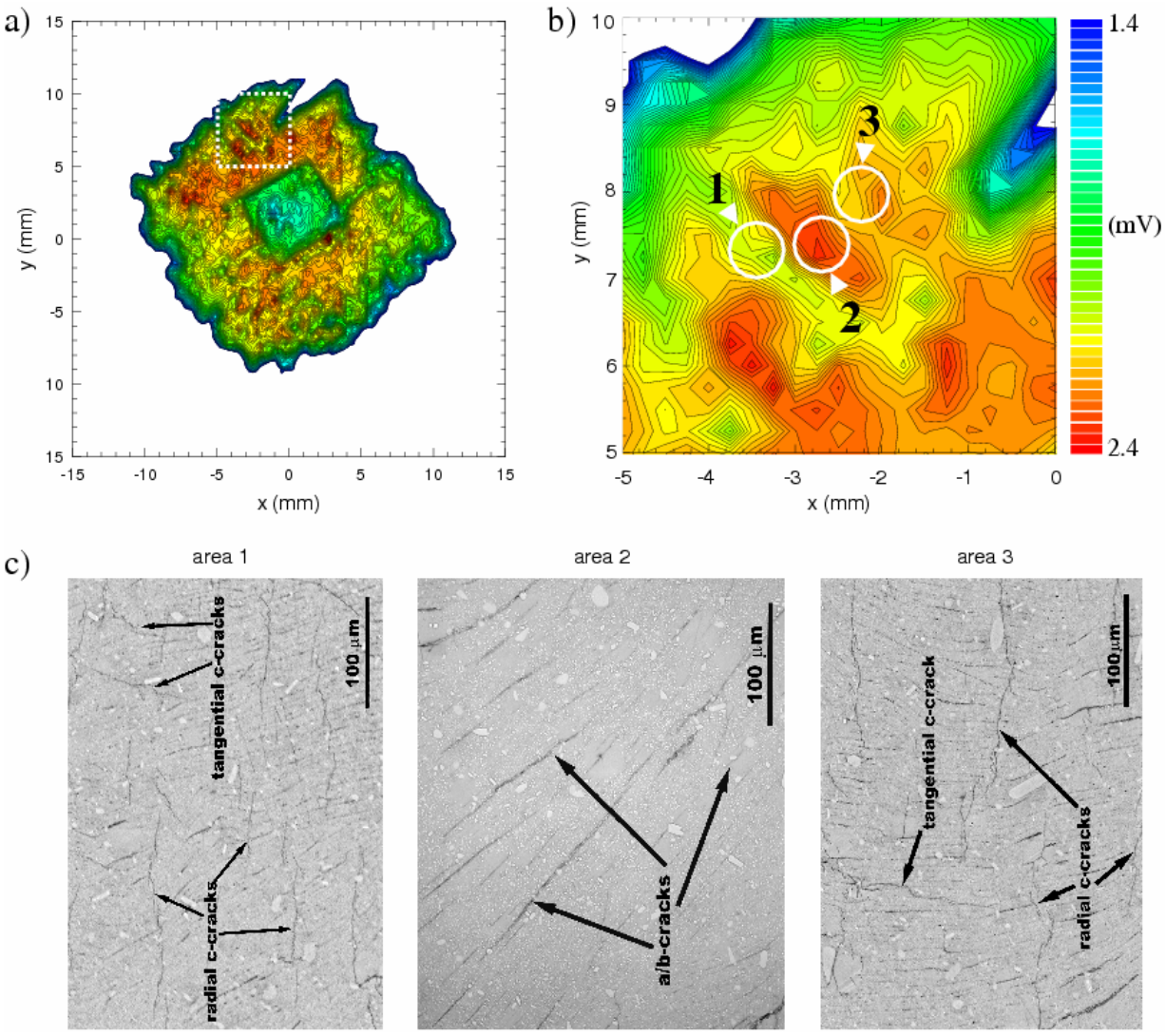

Fig. 3: a) Magnetoscan (original system) of sample *C2*. b) Magnification of the marked region in a). c) Optical micrographs of areas 1-3 as denoted in b) showing the *c*-axis crack distribution.

Given that a survey of the whole sample is very time consuming, one interesting region of the magnetoscan image, such as the top surface of sample *C2* where high and low local supercurrent regions are particularly pronounced, was selected for a detailed microstructural examination. A set of

micrographs was taken from this region with maximum, minimum and medium J_C levels (Fig. 3c). The micrographs (area 1, area 2 and area 3) confirm that the region of minimum J_C contains a high density of radial *c*-axis cracks (i.e. cracks in the *a/c*-plane perpendicular to the relevant *a/c*-growth sector boundary). On the other hand, the region of maximum J_C was crack-free. The region of medium J_C also contains a medium density of radial *c*-axis cracks. Some quantitative results of the *c*-axis crack measurements in areas 1-3 are listed in table 1.

Table 1. Mean values of the *c*-axis crack spacings and lengths in the regions with maximum (area 2), minimum (area 1) and medium (area 3) supercurrent levels measured from the optical micrographs.

REGION	SPACING (μm)		LENGTH (μm)	
	RADIAL	TANGENTIAL	RADIAL	TANGENTIAL
area 1	64	160	96	47
area 2	0	0	0	0
area 3	107	188	79	54

4. Conclusions

Bulk, superconducting samples of YBCO fabricated by top seeded melt growth have been characterized by magnetoscan and optical microscopy. The minima and maxima of the signal measured during the magnetoscan (original design) correspond directly to the magnetoscan (new design) signal and the *c*-axis crack density obtained from optical investigations. Hence it may be concluded that the local supercurrents induced by the small permanent magnet in the magnetoscan are sensitive to the *c*-axis crack network. It has been shown further, that cooling cycles to liquid nitrogen temperature do not introduce new *c*-axis cracks into the large grain microstructure.

Acknowledgments
The experimental work performed at the Atomic Institute, TU Vienna, was supported by the Austrian Science Fund (project no. 17443). The work at the IRC in Superconductivity is supported by the EPSCR. The work at the IEP Košice has been supported by the VEGA project No. 4062, EU Networks SCENET-2 and EFFORT and SAS Centre of Exellence, Nanosmart.

References
[1] P. Diko, Supercond. Sci. Technol. 17 (2004) R45-R58
[2] S. Kracunovska, P.Diko, D. Litzkendorf, T. Habisreuther, J. Bierlich, W. Gawalek, Supercond. Sci. Technol. 18 (2005) S142-S148
[3] M. Eisterer, S. Haindl, T. Wojcik, H. W. Weber, Supercond. Sci. Technol. 16 (2003) 1282-1285
[4] S. Haindl, M. Eisterer, H. W. Weber, L. Shlyk, G. Krabbes, Supercond. Sci. Technol. 18 (2005) S164-S167
[5] S. Haindl, M. Eisterer, H. W. Weber, N. Hari Babu, D. A. Cardwell, IEEE Transactions on Applied Superconductivity 15 (2005) 3129-3132
[6] S. Haindl, M. Eisterer, N. Hörhager, H. W. Weber, H. Walter, L. Shlyk, G. Krabbes, N. Hari Babu, D. A. Cardwell, Physica C 426-431 (2005) 625-631
[7] M. Zeisberger, T. Habisreuther, D. Litzkendorf, A. Surzhenko, W. Gawalek, Supercond. Sci. Technol. 18 (2005) S90-S94
[8] T. Kono, N. Sakai, S. Nariki, I. Hirabayashi, M. Murakami, N. Koshizuka, IEEE Transactions on Applied Superconductivity 15 (2005) 3640- 3643
[9] S. Haindl, Supercond. Sci. Technol. 18 (2005) 1483-1488
[10] G. Krabbes, P. Schätzle, W. Bieger, U. Wiesner, G. Stöver, M. Wu, T. Strasser, A. Köhler, D. Litzkendorf, K. Fischer, P. Görnert, Physica C 244 (1995) 145
[11] M. Zehetmayer, private communication